Conformational Landscape of (*R*,*R*)-Pterocarpans with Biological Activity in Vacuo and in Aqueous Solution (PCM and/or Water Clusters)†

Giuliano Alagona* and Caterina Ghio

CNR−IPCF, Institute for Physical Chemistry Processes, Molecular Modeling Lab, Via Moruzzi 1, I-56124 Pisa, Italy

Received: July 1, 2005; In Final Form: August 9, 2005

All possible combinations of stable dihedral values have been considered in vacuo at the B3LYP/6-31G* level for 3,9-dihydroxy-4,8-diprenylpterocarpan (erybraedin C), whose hydroxy out-out conformation had been examined earlier together with the conformational preferences of 3,9-dimethoxy-4-prenylpterocarpan (bitucarpin A) at the same level (*Phys. Chem. Chem. Phys.* **2004**, *6*, 2849). The structure with O_5 trans with respect to H_{6a} (O_t) is about 2 kcal/mol less stable in vacuo than that with one of the H_6 trans to it (H_t); in aqueous solution its energy gap is nearly conserved. The in-in arrangement of the hydroxyl groups of erybraedin turns out to be preferred in vacuo (even considering zero point and thermal effects), where pseudo H-bonds are formed between hydroxy hydrogens and π electron distributions of prenyl groups. The continuum solvent effect (water) at the IEF−PCM/B3LYP/6-31G* level on the relative stability of the various rotamers is very limited both on bitucarpin and erybraedin. Considering the dihydrated derivatives, significant differences in the solvation energy are found between the distinct hydration sites, increasing in the order: methoxy O, ring O, hydroxy O, and hydroxy H. In hydroxy−water interactions, in fact, water prefers to behave as an H-bond acceptor unless nearby bulky groups prevent its approach. Interestingly enough, a bridging water molecule between the hydroxy H of erybraedin and the prenyl group can be found. The inclusion of BSSE corrections in hydroxy−water interactions decidedly favors out-out hydrated arrangements, followed by out-in and in-out ones. Bulk solvent effects with IEF−PCM about the dihydrated systems almost invert the stability order found in vacuo. When a four−water cluster is considered using QM methods, waters gather in H-bonded pairs around the solute OH groups. MD simulations, carried out on a pterocarpan solute (*J. Phys. Chem. B* **2005**, *109*, 16918), supply water adducts consistent with a liquid state that have also been embedded in the continuum solvent.

I. Introduction

Pterocarpans are ubiquitous in higher plants[1] and play an important role in plant defense (phytoalexins).[2] They are stress-induced low molecular weight antibiotics, protecting plants against fungal infections and pests. Because of their long-renowned antimicrobial, insecticidal, and oestrogenic activities they have been widely used in traditional medicine.[3] Either natural or synthetic products have been shown to possess high antifungal,[4] antibacterial,[5] cytotoxic,[6] and/or anti-HIV[7] activities. Several are potent antidotes against snake and spider venoms.[8] Recently, bitucarpin A (3,9-dimethoxy-4-prenylpterocarpan) and erybraedin C (3,9-dihydroxy-4,8-diprenylpterocarpan) received attention because they exhibit a considerable anticlastogenic activity toward mitomycin C (MMC) and the radio-mimetic bleomycin (BL), used as reference clastogens, whereas when assayed alone they do not affect either the mitotic index or the cell-proliferation index of human lymphocytes.[9] In addition, erybraedin C was found to induce necrosis in leukaemia Jurkat T cells[10] and showed a moderate activity against all cell lines used in that study.[10] They are extracted from plants of the genus *Psoralea* (shown in Figure S1 of the Supporting Information) widely spread in several regions of our planet.

CHART 1: Schematic Structures of Erybraedin C and Bitucarpin A with Their Constituting Chromophores (Chromane and 2,3-Dihydrobenzo[*b*]furan), Where Rotatable Bond Names and Atom Numbering Are Also Indicated

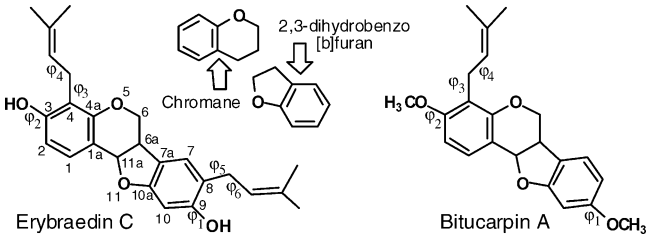

The main structural feature of pterocarpans is the simultaneous presence in their skeleton of two fused chromophores, producing two chiral centers (6a and 11a), shown in Chart 1. Since the distinct peculiar properties of these compounds originate from substitution patterns to the common backbone, a systematic investigation has been initiated considering bitucarpin A and erybraedin C as test cases. All the possible scaffold and side-chain arrangements of bitucarpin A had been examined in vacuo at the B3LYP/6-31G* level.[11] Reference is made to that study as far as configurations, helicity, stabilities and conformer names are concerned. For erybraedin C, only the OH group arrangements consistent with the methoxy ones of bitucarpin A had been considered in ref 11. To complete the

* Corresponding author. Telephone: +39-050-3152450. Fax: +39-050-3152442. E-mail: G.Alagona@ipcf.cnr.it.

† Part of the special issue "Donald G. Truhlar Festschrift".

10.1021/jp053612k CCC: $33.50
Published on Web 10/15/2005

examination of the erybraedin C conformational preferences, in the present study all stable conformations of its hydroxy groups in vacuo have been examined at the same level. Moreover, the solvent effect on internal geometries and relative stabilities has been considered using the polarizable continuum model (PCM)[12] in the IEF framework.[13] The interconversion pathways H_t to O_t (atoms trans to H_{6a} in turn, thus producing inversion in the ring system helicities), studied in vacuo on a model system in ref 11, have been now considered for bitucarpin A and erybraedin C in vacuo and in solution.

Small water clusters[14] have been in addition taken into account to evaluate the capabilities as H-bond acceptors of the different ethereal oxygens in bitucarpin and to assess the preferential H-bonding pattern of the hydroxy groups of erybraedin, in comparison to the ring ethereal groups as well, in the gas phase and in the presence of the continuum solvent. This hybrid approach should allow reliable estimates of specific H-bonding interactions (absent from a pure continuum calculation with a protic solvent) and bulk solvent effects on the solute's structure and stability, especially in the case less acidic HX subunits are considered.[16]

II. Computational Details

Beside the backbone arrangement and the (6a, 11a) chirality, the structures of the two pterocarpans under investigation are characterized by the side chain orientations, determined by the φ_1 ($C_{10}C_9OX$) and φ_2 (C_2C_3OX) with X = methyl (Me) or H, φ_3 (C_3C_4CC), φ_4 (C_4CCC), and φ_5 (C_9C_8CC), φ_6 (C_8CCC) where applicable, dihedral angles, as shown in Chart 1. In the present study, the cis(6a*R*, 11a*R*) configuration is considered, taking into account also the H_t and O_t conformations of the backbone (H_t and O_t indicate which atom is trans to H_{6a}). When not otherwise specified, the H_t arrangement is considered.

A. In Vacuo Geometry Optimizations. The minimum energy OH arrangements for erybraedin have been determined fully relaxing the structures at the DFT level by applying the B3LYP functional[17] and the 6-31G* basis set[18] in the gas phase with the Gaussian 03 system of programs,[19] using the 1998 constants. φ_1 ($C_{10}C_9OH$) and φ_2 (C_2C_3OH) values in the vicinity of the minima determined for 3,9-dihydroxypterocarpan in ref 11 were adopted for initial geometries, with prenyl side chains in 16 possible different arrangements, i.e., φ_3 and φ_5 in the $\pm 90°$ regions, and φ_4 and φ_6 in the $\pm 120°$ regions, corresponding to the most stable positions in vacuo of a prenyl side chain in pterocarpans. All Hessian matrix eigenvalues were positive for local minima (only one eigenvalue was negative for TS) in converged GDIIS[20] geometry optimizations. However, a number of frequency calculations at the B3LYP/6-31G* level were carried out for control, confirming all stationary points found. Zero point and thermal corrections, computed at $T = 298$ K and $p = 1$ atm in the rigid rotor-harmonic oscillator approximation[21] to obtain free energies, are reported relative to a reference conformer:

$$\Delta G_g = \Delta E_g + \Delta \mathrm{ZPE} + \Delta H(T) - T\Delta S(T) \qquad (1)$$

where ΔE_g is the relative gas-phase energy at 0 K and ΔZPE (unscaled since its B3LYP/6-31G* proposed scaling factor is very close to unity) is the relative vibrational energy at 0 K, while $\Delta H(T)$ and $\Delta S(T)$ are the relative changes in enthalpy and entropy going from 0 to T K.

The φ_1,φ_2 potential energy surface (PES) was computed, starting from the lowest energy structure of erybraedin, employing the flexible surface scan algorithm in Gaussian (all degrees of freedom are allowed to relax but φ_1 and φ_2). Problems encountered are discussed in the suitable location.

A few B3LYP/6-311++G**[18] single point calculations (834 contracted basis functions) have been carried out on the B3LYP/6-31G* optimized geometries in order to evaluate the basis set effect. [The 6-31G* erybraedin description already consists of 491 contracted basis functions.]

B. Geometry Optimizations in the Continuum Solvent. The integral-equation-formalism (IEF)-PCM method,[13] as implemented in Gaussian 03, has been employed still at the B3LYP/6-31G* level, using gas-phase optimized geometries as starting structures, where appropriate. The advantage of the IEF−PCM approach with respect to standard PCM, beside computational efficiency, is that errors, such as those ascribable to the partition of the continuous apparent surface charge into discrete elements and to the electronic charge escaped outside the cavity, are reduced at least by an order of magnitude, because of the use of operators related to the electric potential instead of the electric field.[22] The cavity of interlocking spheres around the solute was built using a united atom description for the CH (R = 1.9 Å) and CH_2/CH_3 (R = 2.0 Å) groups. Bondi radii[23] have been employed for oxygen, acidic H, and the remaining carbon atoms. All radii (united or not) were scaled by a factor of 1.2. For the sake of clarity, the quantities reported in the tables are summarized hereafter.

The IEF−PCM free energies were calculated as

$$G_{tot} = E^s_{int} + {}^1/_2 E_{susv} + G_{drc} = G_{es} + G_{drc} \qquad (2)$$

where the first two terms, i.e., the internal energy of the fully polarized solute in solution and the solute−solvent (susv) interaction, correspond to the electrostatic contributions (es) to the free energy of the solute in solution, while G_{drc}, namely dispersion−repulsion−cavitation, corresponds to the nonelectrostatic ones.

The relative values are calculated with respect to the reference conformer ones, reported at their first occurrence:

$$\Delta G_x(\mathrm{i}) = G_x(\mathrm{i}) - G_x(\mathrm{ref}) \qquad (3)$$

The electrostatic and total solvent effects, $G^{es}(sol)$ and $G^{tot}(sol)$, are computed for each conformer with respect to its optimized geometry in the gas phase (E_g):

$$G^x(\mathrm{sol})(\mathrm{i}) = G_x(\mathrm{i}) - E_g(\mathrm{i}) \qquad (4)$$

with x standing in both equations for es or tot.

C. Supermolecule Calculations. Supermolecules with from 2 up to 4 water molecules added in the vicinity of specific H-bonding sites around the solute have been considered as well either in vacuo or in the presence of a continuum solvent. A random selection has been made of local minima, although preference was given with few exceptions to the most stable conformers of each kind among those considered.

A few brief definitions of the energetic terms follow to help in understanding the table content. The hydration energy of the i solute is defined as

$$E_{hydr}(\mathrm{i}) = E(\mathrm{i,hydr}) - E_g(\mathrm{i}) - n\,E_g(H_2O) \qquad (5)$$

where E(i,hydr) is the internal energy of the system, made up of the i solute and n water molecules nearby; E_g indicates the gas-phase internal energy of the isolated species; thus, E_{hydr}(i) is the interaction energy of i with n water molecules, including geometry deformation effects and water mutual interactions.

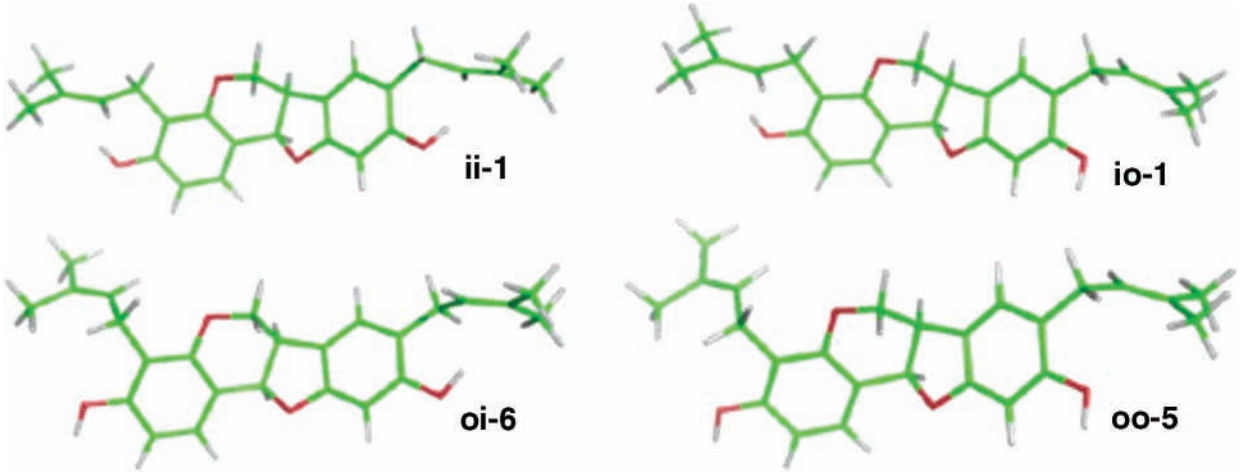

Figure 1. B3LYP/6-31G* lowest energy structures for each orientation (φ_1,φ_2) of the hydroxy groups in erybraedin C: ii [180°,180°], io [0°,180°], oi [180°,0°], and oo [0°,0°]. The ii-1 structure, with both hydroxy hydrogens pointing toward the π density of the prenyl double bonds, is the lowest energy one in vacuo.

The differential solvent effect is measured with respect to the reference system, taken as zero:

$$\Delta(\text{solv eff})(\text{i}) = E_{\text{hydr}}(\text{i}) - E_{\text{hydr}}(\text{ref}) \quad (6)$$

while the relative energy of hydration, ΔE_{hydr}(i), includes the stability in the gas phase of the i system:

$$\Delta E_{\text{hydr}}(\text{i}) = E(\text{i,hydr}) - E(\text{ref,hydr}) = \Delta(\text{solv eff})(\text{i}) + \Delta E_{\text{g}}(\text{i}) \quad (7)$$

Counterpoise (CP) corrections have been considered using the Boys−Bernardi method,[24] with the basis set superposition errors (BSSE) directly defined as $\Delta E - \Delta E^{\text{CP}}$, according to Sokalski et al.[25] The uncorrected reference energy does not refer, however, to the isolated systems, as in eq 5, but to the 3-component system in the adduct geometry, as the corrected one.[26] Therefore:

$$\text{BSSE}(\text{i}) = \Delta E(\text{i}) - \Delta E^{\text{CP}}(\text{i}) = E_{\text{hydr}}(\text{i}) - E^{\text{CP}}_{\text{hydr}}(\text{i}) \quad (8)$$

III. Results and Discussion

A. Erybraedin C Local Minima in the Gas Phase Depending on OH Group Arrangements. The conformational properties of each hydroxy group, thoroughly examined at the B3LYP/6-31G* level in vacuo for a fixed starting orientation of the other OH group in the case of 3,9-dihydroxypterocarpan (named Ptero for short), produced four rotamers with relative stabilities within 0.3 kcal/mol of the most stable one (either for the H_t or O_t backbone arrangement) corresponding to $\varphi_1 \approx 0°$ and $\varphi_2 \approx 180°$, thus indicated as 0°,180°.[11] The 180°,180° conformer was almost as stable as the 0°,180° one. Analogously the 0°,0° and 180°,0° couple turned out to be very close in energy, but ~0.2 kcal/mol higher than the previous one. In contrast, in erybraedin C, the structure and stability of the OH group rotamers, named hereafter for short oo [0°,0°], ii [180°,180°], oi [0°,180°], and io [180°,0°], are possibly affected by the presence of vicinal prenyl groups. Because the conformational flexibility of a prenyl side chain gives rise to four local minima with $\varphi_3 \approx \pm 90°$ and $\varphi_4 \approx \pm 120°$,[11] a similar behavior could be expected for the second prenyl side chain as well, although located at C_8 (C_{10} actually should be more consistent with C_4). Therefore, 16 minima might be located for each OH group rotamer, unless steric hindrance or unfavorable electrostatic interactions prevent peculiar structures from existing. Nonetheless, particular attention must be paid to starting geometries not to miss several conformers, especially in the case of the ii family.[27]

TABLE 1: B3LYP/6-31G* Relative Stabilities (ΔE_g, in kcal/mol) of the Optimized Local Minima of Erybraedin C, with Respect to ii-1[a]

	ii	oi	io	oo
1	0[b] (0[c])	2.23 (1.60)	2.10 (1.74)	4.39 (3.51)
2	0.02 (0.01)	2.21 (1.66)	2.13 (1.78)	4.39 (3.36)
3	2.95	5.15	2.16	4.40
4	2.98	5.15	2.18	4.42
5	0.07	2.04	2.16	4.22
6	0.10	2.04	2.19	4.24
7	2.99	4.99	2.20	4.25
8	2.99	5.01	2.19	4.26
9	2.64	2.14	4.76	4.29
10	2.63	2.14	4.80	4.33
11	5.57	5.05	4.78	4.34
12	5.58	5.08	4.81	4.31
13	2.72	2.25	4.85	4.38
14	2.73	2.21	4.84	4.38
15	5.66	5.17	4.88	4.41
16	5.68	5.17	4.90	4.44

[a] In parentheses, single point B3LYP/6-311++G**//B3LYP/6-31G* relative stabilities. [b] The B3LYP/6-31G* reference energy is −1270.389431E_h. [c] The B3LYP/6-311++G**//B3LYP/6-31G* reference energy is −1270.738544E_h.

The 16 structures, numbered from 1 to 16, have been gathered in four sets, each corresponding to analogous ranges of values for the φ_3 and φ_4 dihedral angles (namely, 1−4, $\varphi_3 > 0°$, $\varphi_4 < 0°$; 5−8, $\varphi_3 < 0°$, $\varphi_4 > 0°$; 9−12, $\varphi_3 < 0°$, $\varphi_4 < 0°$; 13−16, $\varphi_3 > 0°$, $\varphi_4 > 0°$), while within each set they are ordered depending on the ranges of the φ_5 and φ_6 dihedral angles (I, $\varphi_5 > 0°$, $\varphi_6 < 0°$; II, $\varphi_5 < 0°$, $\varphi_6 > 0°$; III, $\varphi_5 > 0°$, $\varphi_6 > 0°$; IV, $\varphi_5 < 0°$, $\varphi_6 < 0°$). This ordering allows a quick recollection of prenyl group orientations. Reference is made to the structures using a type-order code, as shown in Figure 1, where the lowest energy structures for each distinct arrangement of the OH groups are displayed (Cartesian coordinates are at the end of the Supporting Information).

From the relative energies of stable conformers (reported in Table 1), determined for each prenyl group position with respect to the lowest energy rotamer (ii-1), a wide variability in the hydroxy group conformer stabilities depending on the prenyl side chain arrangements can be observed (torsional parameters in Tables S1−S4 of the Supporting Information for ii, oi, io, and oo, respectively).

TABLE 2: B3LYP/6-31G* Relative Stabilities for Some Local Minima of Erybraedin C in the Gas Phase Corrected with the Addition of the Individual Terms of Eq 1, Including Zero Point Energies, Thermal Corrections to the Enthalpy, and Finally Entropic Terms To Obtain Relative Free Energies (kcal/mol)[a]

	ΔE_g	$+\Delta$ZPE	$+\Delta H_{th}$	ΔG_g
ii-1	0	0[b]	0[c]	0[d]
ii-2	0.024	−0.019	−0.015	−0.073
io-1	2.235	2.078	2.187	1.827
io-2	2.208	2.061	2.160	1.782
oi-1	2.103	1.980	2.072	1.775
oi-2	2.129	1.953	2.064	1.628
oo-1	4.387	4.064	4.296	3.045
oo-2	4.392	4.084	4.298	3.487
oo-5	4.216	3.840	4.088	2.904
oo-6	4.241	3.916	4.136	3.277
oo-7	4.250	3.930	4.158	3.018
oo-8	4.263	3.933	4.153	3.098

[a] Each term includes all the previous ones according to eq 1; this allows an immediate comparison between the various corrected stabilities. Reference values (in E_h) for ii-1 are: [b] Up to ZPE = −1269.910655. [c] Up to enthalpy = −1269.882067. [d] G_g = −1269.970147.

The relative stabilities range from 0 to 5.7 kcal/mol, with rotamers ii-2, -5, and -6 within 0.1 kcal/mol of ii-1 at most, while rotamers ii-9, -10, -13, -14, -3, -4, -7, and -8 in that order are 2.6−3 kcal/mol higher in energy. The least stable rotamers (11, 12, 15, 16) belong to the ii group because of electrostatic repulsion and steric hindrance. In the oi family the most stable rotamers (around 2.0−2.2 kcal/mol) are oi-1, -2, -5, -6, -9, -10, -13, and -14, while the remaining ones range from 5.0 to 5.2 kcal/mol. In the io family as well there are just two different and narrow ranges of stability: 2.1−2.2 and 4.8−4.9 kcal/mol for rotamers 1−8 and 9−16, respectively. Finally, in the oo family the stability of all the rotamers is very similar and confined in the interval 4.2−4.4 kcal/mol. The basis set effect (the values in parentheses in Table 1 have been computed with the B3LYP/6-311++G** basis set on the B3LYP/6-31G* optimized geometries) does not modify the situation: high-energy conformers are just somewhat stabilized with respect to the most stable ones.

Considering zero point and thermal corrections for selected conformers leaves the overall picture unaltered as well (see Table 2) although remarkable changes are found in the relative free energies especially for the oo rotamers. The inversion in the stabilities of ii-1 and ii-2 refers to total gaps by less than 0.1 kcal/mol. Zero point effects slightly reduce the energy gaps with respect to ii-1, whereas thermal corrections to the enthalpy tend to counterbalance them. The main contribution is due to the entropy term that stabilizes the higher energy rotamer with respect to ii-1. However, all low-frequency modes have been taken as vibrations whereas some of them could be considered as hindered rotations.

To appreciate the erybraedin flexibility in vacuo, the full φ_1,φ_2 PES, displayed in Figure 2, has been computed from different starting points ($\varphi_1 = \varphi_2 = -180°$ and $\varphi_1 = \varphi_2 = 180°$) in ±30° increments using as initial values of the other torsions those corresponding to ii-1.

Interestingly enough, starting from $\varphi_1 = \varphi_2 = -180°$, the prenyl side chains move somewhat away from their initial position and are unable to return to the best orientation when φ_2 reaches 30° (regardless of the $\varphi_1$value). In contrast, starting from $\varphi_1 = \varphi_2 = 180°$, the prenyl side chains keep an arrangement close to the initial one, allowing the structure to resume the lowest energy conformation. The map has been drawn starting from $\varphi_1 = \varphi_2 = 0°$ because the low energy basins

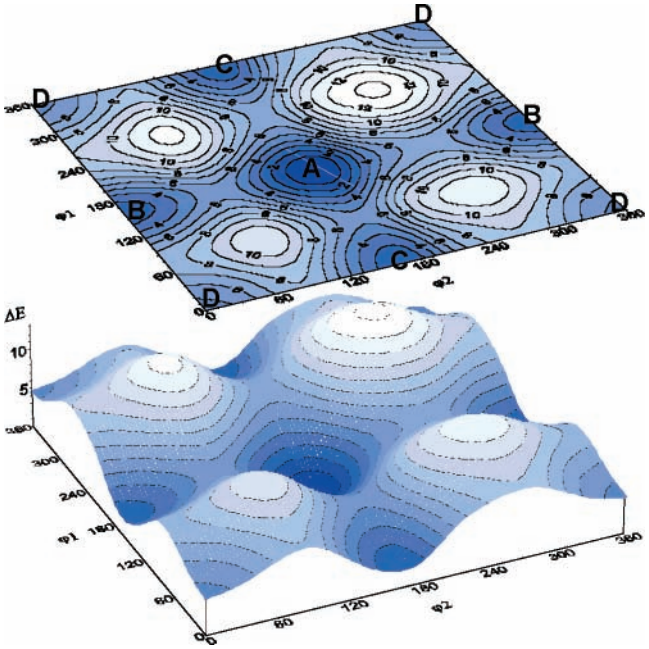

Figure 2. B3LYP/6-31G* φ_1,φ_2 potential energy surface for (*R*,*R*)-erybraedin C in vacuo. The low energy structures are indicated on the map, drawn with respect to ii-1, taken as zero.

TABLE 3: B3LYP/6-31G* Relative Stability with Respect to ii-1 (kcal/mol) and Geometric Parameters (deg) of the Optimized Transition States of (*R*,*R*)-Erybraedin C

	ΔE_g	φ_1	φ_2	φ_3	φ_4	φ_5	φ_6
TS_{BA}	5.56	161.4	81.9	85.4	−116.6	56.9	−132.8
TS_{AB}	6.51	161.3	266.5	105.2	−105.8	57.2	−132.7
TS_{CA}	6.70	262.9	164.2	52.8	−132.0	96.4	−112.1
TS_{AC}	5.15	78.3	164.7	52.1	−132.5	75.9	−118.8
TS_{DB}	8.90	264.2	0.8	95.2	−114.5	84.1	−116.9
TS_{BD}	7.46	78.0	0.9	97.4	−113.4	74.6	−119.4
TS_{DC}	7.71	−0.02	81.2	84.1	−117.3	81.7	−118.9
TS_{CD}	8.63	−0.3	266.6	105.0	−106.3	82.5	−118.5

are cut in an almost symmetric way, due to the lack of steric hindrance when φ_1 and/or φ_2 are close to 0°. Conversely, when in the 180° region, stable arrangements show φ_1 or φ_2 values about 160°. As expected from the results obtained considering all the possible combinations of the φ_1, φ_2, φ_3, φ_4, φ_5, and φ_6 dihedral angles, four types of minima (named A, B, C, D), roughly corresponding to ii, oi, io, and oo, respectively, have been located on the PES. Four rotational transition states can be found in the inner part of the map along the lines joining A either to B (TS_{BA}, TS_{AB}) or C (TS_{CA}, TS_{AC}),[28] and also along the borders joining D either to B (TS_{DB}, TS_{BD}) or C (TS_{DC}, TS_{CD}).[29] TS geometry optimizations, starting from the closest points on the map, produced the structures reported in Table 3.

Of course, this picture is related to a particular arrangement of the prenyl side chains, but it is likely that analogous results are obtained for other arrangements, although shifted according to the relative stabilities of the peculiar structures.

B. Bitucarpin A. Four local minima had been found for (*R*,*R*)-bitucarpin A, depending on the prenyl side chain orientations, as already recalled. In what follows, they are named Bitu 1, Bitu 2, Bitu 3, and Bitu 4 and correspond respectively to (φ_3,φ_4)/ΔE (kcal/mol) values of (−81.4°,−114.1°)/0; (−98.9°,+114.3°)/0.02; (82.1°,115.9°)/0.11; (+94.9°,−155.0°)/0.21, all with the φ_1 and φ_2 torsions close to 0°.[11]

C. H_t and O_t Backbone Structures *in Vacuo* and in Solution for Erybraedin and Bitucarpin. *1. In vacuo.* The H_t to O_t interconversion PES computed on (*R*,*R*)-3,9-dihydroxy-

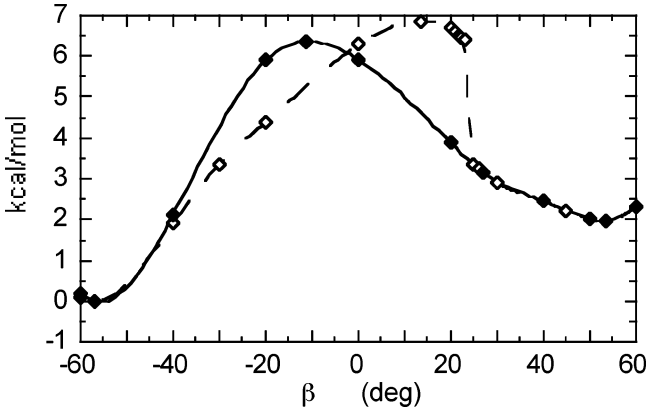

Figure 3. B3LYP/6-31G* potential energy profile for the H_t/O_t interconversion of Bitu 1 in the gas phase, computed in both forward (−60° to +60°, dashed line) and backward (solid line) directions.

TABLE 4: B3LYP/6-31G* Relative Stability (kcal/mol) of H_t and O_t Minima and Transition States Joining Them for Bitucarpin A and Two Minima of Erybraedin C as Compared to 3,9-Dihydroxypterocarpan (Ptero)[a]

	H_t	O_t	TS1	TS2
Ptero 0°,180°	0[b] (−56.8)	1.97 (53.4)	6.27 (−9.1)	6.80 (12.0)
Bitu 1	0[c] (−56.8)	1.95 (53.4)	6.35 (−11.1)	6.85 (13.4)
Eryc ii	0 (−57.4)	1.99 (53.8)	6.45 (−10.8)	7.03 (14.1)
Eryc oo	4.22 (−57.0)	6.16 (53.1)	10.56 (−10.4)	11.11 (12.9)

[a] The value of β ($C_{11a}C_{6a}C_6O_5$) in degrees is indicated in parentheses. [b] The Ptero H_t reference energy is $-879.696408E_h$. [c] The Bitu 1 H_t reference energy is $-1153.651967E_h$.

pterocarpan [with $\varphi_1,\varphi_2 = 0°,180°$] as a model system, displayed in ref 11 using β ($C_{11a}C_{6a}C_6O_5$) and α ($C_1C_{1a}C_{11a}O_{11}$) as leading parameters, is only slightly affected by prenyl side chains at C_4 and C_8 or when two methoxy groups replace the hydroxy ones in the presence of a vicinal (at C_4) prenyl side chain. The trend of the forward (β varying from −60° to +60° in variable intervals) and backward energy profiles for the H_t/O_t interconversion, shown in Figure 3 for Bitu 1, is almost indistinguishable from the Eryc one and compares well with Figure 4 of ref 11.

The computation of energy profiles, carried out at fixed values of β, produces the drift from one path to the other because of the shape of the α,β PES: when hops are present, the α values of adjacent points refer to different regions of the PES, as already stressed.[11] Thus, the energy profiles do not coincide with either interconversion pathway. By imposition of a pair of dihedral values, like in a potential energy grid, this drift is prevented, but many more points, if not the whole surface, should be computed. Despite the significant differences in the pterocarpans here considered, not only the shape of the profiles but also the mutual values of the stationary points on the relevant PES are conserved. The relative stabilities of H_t, O_t, TS1, and TS2 are reported in Table 4 together with the corresponding β value.

Interestingly enough, the mutual stabilities of the stationary points in Eryc oo are closer to those of Bitu 1 than to those of Eryc ii, probably because of the similar orientation of the OX groups.

2. In Aqueous Solution. The solvation properties of the H_t and O_t forms of bitucarpin A and erybraedin C have been investigated carrying out geometry optimizations in water (ϵ = 78.39) at the B3LYP/IEF−PCM/6-31G* level starting from the structures optimized in vacuo. From the values reported in Table 5 for selected conformers, it is evident that the continuum solvent effect on the relative stability of the various forms is very limited.

TABLE 5: B3LYP/IEF−PCM/6-31G* Free Energy of Solvation and Solvent Effects (kcal/mol) on the H_t and O_t Minima of Selected Stable Conformers and TS (from Table 4) of Bitucarpin A and Erybraedin C[a]

	ΔE_g	$^1/_2E_{susv}$	G^{es}(sol)	G^{tot}(sol)	ΔG_{es}	ΔG_{tot}
Bitu 1 H_t	0	−8.23	−7.20	1.05	0[b]	0[c]
Bitu 2 H_t	0.02	−8.31	−7.28	0.89	−0.06	−0.13
Bitu 3 H_t	0.11	−8.29	−7.25	1.11	0.06	0.17
Bitu 4 H_t	0.21	−8.33	−7.30	0.99	0.11	0.15
Eryc ii H_t	0	−10.39	−9.02	−0.40	0[d]	0[e]
Eryc oi H_t	2.04	−11.44	−9.95	−0.47	1.11	1.97
Eryc io H_t	2.10	−10.65	−9.48	−0.18	1.64	2.32
Eryc oo H_t	4.22	−11.82	−10.51	−0.38	2.73	4.24
Eryc ii O_t	1.99	−11.49	−9.74	−0.55	1.27	1.85
Eryc oo O_t	6.16	−12.71	−11.08	−0.09	4.10	6.47
Bitu 1 O_t	1.95	−9.16	−7.84	1.22	1.31	2.12
Bitu 2 O_t	1.95	−9.22	−7.90	0.99	1.25	1.89
Bitu 3 O_t	2.00	−9.06	−7.73	1.63	1.47	2.58
Bitu 4 O_t	2.12	−9.38	−8.01	0.75	1.31	1.82
Bitu 1 TS1	6.35	−8.99	−7.70	0.63	5.85	5.93
Bitu 1 TS2	6.85	−8.47	−7.36	1.36	6.69	7.16
Eryc ii TS1	6.45	−11.12	−9.46	−0.72	6.01	6.13
Eryc ii TS2	7.03	−10.82	−9.27	−0.03	6.79	7.40
Eryc oo TS1	10.56	−12.51	−10.91	−0.62	8.66	10.34
Eryc oo TS2	11.11	−11.92	−10.55	0.06	9.59	11.58

[a] G_{drc} can be derived for each conformer from the difference between the relevant G^{tot}(sol) and G^{es}(sol) values. [b] The reference electrostatic free energy is $-1153.663438E_h$. [c] The reference total free energy is $-1153.650290E_h$. [d] The reference electrostatic free energy is $-1270.403806\ E_h$. [e] The reference total free energy is $-1270.390074E_h$.

Only the electrostatic terms show some change, although almost completely counterbalanced by cavitation, dispersion, and repulsion contributions, leaving the relative free energy ordering practically unaltered. As a common feature, the electrostatic solvent effect is somewhat weaker in bitucarpin than in erybraedin, thus producing a slightly unfavorable total solvent effect. In contrast, in erybraedin, it turns out to be generally favorable, even though vanishingly small.

To understand the reason the electrostatic part of the continuum solvent effect is so feeble in these systems, dipole moments of the main families have been computed, because the solvent reaction field, closely related to the solute molecular electrostatic potential (MEP), displayed in Figure S2 of the Supporting Information, is stronger when dominated by a dipolar component than by a quadrupolar one.[30] Rather than the value of the moment itself, its orientation is important. In the case of Bitu 1−4 the magnitude of μ ranges from 2.15 to 2.55 D, with a nearly constant orientation, and the solute MEP has a remarkable quadrupolar component (Figure S2a). Therefore, in this system, no large differential solvation effect can be expected. In contrast, in erybraedin the dipole moment orientation varies depending on the OH group arrangements. When both hydroxy hydrogens point inward (Eryc ii), μ is directed along the $C_{11a}-C_{6a}$ axis with a value of 5.8 D, and the solute MEP is dominated by the dipolar component (Figure S2b). Conversely, in Eryc oo, μ is directed in the opposite direction, with a magnitude of 2.6 D, and the solute MEP presents a complex pattern (Figure S2c), hard to decipher. The magnitude of μ is analogous in Eryc oi (2.6 D) and in Eryc io (2.9 D) with orientation nearly parallel to the inward OH group in both cases. Nevertheless, the solvent electrostatic effect is just somewhat larger (by 2−3 kcal/mol) than in bitucarpin.

D. Addition of Explicit Water Molecules. Discrete-continuum approaches successfully reproduce spectroscopic properties[31] as well as hydration free energies.[32] Considering

TABLE 6: B3LYP/6-31G* Hydration Energy, Differential Solvent Effect and Relative Energy of Hydration (kcal/mol) for a Water Molecule per Each Methoxy O of Bitucarpin A[a]

	ΔE_g	E_{hydr}	Δ(solv eff)	ΔE_{hydr}
Bitu 1u	0	−12.14	0.56	0.56
Bitu 1d	0	−12.70	0	0[b]
Bitu 2u	0.02	−13.11	−0.41	−0.39
Bitu 2d[c]	0.02	−13.10	−0.40	−0.38
Bitu 3u	0.11	−12.82	−0.12	−0.01
Bitu 3d	0.11	−12.76	−0.06	0.05
Bitu 4u[c]	0.21	−13.20	−0.50	−0.29
Bitu 4d	0.21	−12.49	0.21	0.42

[a] Structures displayed in Figure S3 of SI. [b] Reference energies $E_{hydr} = -1306.490564E_h$; $E_g(H_2O) = -76.408954E_h$. [c] The water molecule at O_3 moves toward the prenyl π density (see text).

TABLE 7: B3LYP/6-31G* Hydration Energy, Differential Solvent Effect and Relative Energy of Hydration (kcal/mol) for a Water Molecule per Each Ring O of Bitucarpin A[a]

	ΔE_g	E_{hydr}	Δ(solv eff)	ΔE_{hydr}
Bitu 1b	0	−16.54	0	0[b]
Bitu 2b	0.02	−15.56	1.00	0.97
Bitu 3b	0.11	−14.63	2.02	1.91
Bitu 4b	0.21	−14.62	2.13	1.92
Bitu 1bu	0	−15.38	1.15	1.15
Bitu 2bu	0.02	−15.21	1.35	1.33
Bitu 3bd	0.11	−13.99	2.66	2.55
Bitu 4bd	0.21	−13.99	2.76	2.55
Bitu 1a(r)	0	−15.73	0.81	0.81
Bitu 1a(l)	0	−16.09	0.44	0.44

[a] Structures displayed in Figure S4 of SI. [b] Reference $E_{hydr} = -1306.496226E_h$.

that explicit water molecules should play a prominent role in the solvation of these compounds, their capability to form H-bonding complexes at various interaction sites has been analyzed at the B3LYP/6-31G* level, allowing the geometry of the whole system to relax. H-bond donor and acceptor groups were considered separately.

(1) Addition of Two Water Molecules to Bitucarpin A: a. One Water Molecule per Methoxy Group. To explain the hydration positions without showing a large amount of figures (some are displayed in the Supporting Information), reference is made to the Chart 1 views. Since there are two O lone pairs per methoxy group (named u/d according to their upward/downward position with respect to the observer), either the u or d point of attack for water has been considered concerning the methoxy group at C_3. Conversely, due to lack of bulky substituents nearby, the water molecule near the methoxy group at C_9 invariably roughly aligns one of its OH groups along the bisector of the O_9 lone pairs with its free H pointing upward, regardless its starting arrangement. The hydration energies, reported in Table 6 together with the differential solvent effects and the relative energies of hydration, have been computed for the most stable conformers of bitucarpin. For the sake of comparison, the relative stabilities in the gas phase are also reported.

As stated above, distance (1.99 Å) and orientation of the water molecule bound to the methoxy O at C_9 are well conserved. The largest changes are found for the water molecule in the vicinity of the methoxy O at C_3 due to the presence of the prenyl side chain. In two cases (Bitu 2d and 4u) actually, because of the prenyl side chain leaning toward the methoxy group either below or above the backbone plane, the water molecule moves away from the methoxy O lone pair and toward the π density (with $H_w\cdots CH$ and $H_w\cdots C(Me)_2 = 2.7$ and 2.6 Å, respectively, CH and $C(Me)_2$ standing for the double bond C atoms). The $H_w\cdots O_3$ separation and the $O_wH_wO_3$ angle (same H_w as above) become 2.4 Å and 124° in both Bitu 2d and Bitu 4u, indicating a preference for the prenyl group; the other water H points upward in Bitu 2d and downward in Bitu 4u. On the other hand, in the most favorably hydrated structure (Bitu 2u) for instance, the $O_3\cdots H_w$ separation is 1.93 Å with respect to an $O_9\cdots H_w$ value of 1.99 Å. The orientation of water, even when H-bonded to O_3, is remarkably different from that at O_9.

b. One Water Molecule per Ring O. The results related to the hydration on the ethereal O belonging to the rings can be found in Table 7.

In the b series, both water molecules are bound to the O lone pairs pointing below the scaffold plane, i.e., on the same side as the hydrogens bound to the chiral carbon atoms (see structures in Figure S4 of the Supporting Information). The most favorable results, listed in the first group, are obtained when the free H of the water molecule at O_5 points downward and that at O_{11} points upward. Both free water hydrogens point upward in the bu series (downward in the bd one). In 1a, the water molecule at O_{11} is bound to the O lone pair above the scaffold plane (almost perpendicular to it, with its free H toward the right (r) or left (l) hand side, i.e., toward the 2,3-dihydrobenzo[*b*]furan or chromane moiety), while the water molecule at O_5 is still below the scaffold plane.

Ring O···water interactions are in general more favorable than the methoxy O···water ones. Nonetheless their stabilizing effect is consistent with the gas-phase stability and enhances the energy differences. Structures with the free H of water pointing downward (3bd and 4bd) show $H_w\cdots O_{11}$ separations slightly longer and are less stable by about 0.6 kcal/mol than 3b and 4b. Distance (about 1.93 Å) and orientation of the water molecule H-bonded to O_{11} are well conserved in all the other b series.[33]

As expected, the largest changes are related to the water molecule bound to O_5, because of the presence of the prenyl side chain π density. In the case of the most favorably hydrated structure (Bitu 1b), the $O_{11}\cdots H_w$ separation is 1.93 Å with respect to an $O_5\cdots H_w$ distance of 2.11 Å, while the $O_5H_wO_w$ angle is farther from 180° than $O_{11}H_wO_w$.

(2) Addition of Two Water Molecules to Erybraedin C. In the case of erybraedin as well, the most stable structures out of the 16 ones per each type of OH arrangements have been examined.

a. One Water Molecule per Ring O. The hydration energies in erybraedin (ranging from −13.3 to −15.7 kcal/mol), displayed with other quantities in Table 8, are fairly comparable to those in bitucarpin (−14.0 to −16.5 kcal/mol). Ring O···water interactions are thus nearly as favorable as those occurring in bitucarpin. During the optimizations the water molecules move to the lone pair below the scaffold plane, even starting H-bonded to the O lone pairs above the plane. As a general feature, the $O_nH_wO_w$ arrangements (with $n = 5$ or 11) are almost linear (structures displayed in Figure S5 of the Supporting Information). The hydration stabilizing effect is significant when the hydroxy group at C_3 points outward (oi and oo). Because of the high internal energy of these structures in the gas phase, however, the oi complexes turn out to be 0.7 to 0.9 kcal/mol less stable than ii, while the oo ones remain the least favorable among the structures here considered.

Despite the common type (bu) with both free hydrogens pointing upward, those complexes correspond to similar arrangements only in couples. In the ii bu and io bu adducts, for instance, $O_5\cdots H_w \approx O_{11}\cdots H_w \approx 1.95$ Å with $C_4O_5H_wO_w = -133°$ and $C_{10a}O_{11}H_wO_w = 160°$. Conversely, in the oi bu and oo bu adducts, the H-bonding hydroxy group of water is almost

TABLE 8: B3LYP/6-31G* Hydration Energy, Differential Solvent Effect, and Relative Energy of Hydration (kcal/mol) for a Water Molecule per Each Ring O for the Most Stable Conformers in Vacuo of Erybraedin C Where BSSE and Counterpoise Corrected Relative Energies of Hydration Are Also Reported[a]

	ΔE_g	E_{hydr}	Δ(solv eff)	ΔE_{hydr}	ΔE^{CP}_{hydr}	−BSSE
Eryc ii bu	0	−13.91	0	0[b]	0[c]	7.58
Eryc oi bu	2.04	−15.24	−1.33	0.71	0.89	7.77
Eryc io bu	2.10	−13.66	0.25	2.35	2.36	7.59
Eryc oo bu	4.22	−15.08	−1.17	3.05	3.29	7.83
Eryc ii b	0	−13.90	0.01	0.01	−0.67	6.91
Eryc ii b−	0	−13.43	0.48	0.48	0.43	7.53
Eryc oi b	2.04	−15.72	−1.81	0.23	1.03	8.39
Eryc oi bd	2.04	−15.07	−1.16	0.88	1.05	7.76
Eryc io b−	2.10	−13.26	0.65	2.75	2.74	7.58
Eryc oo bd	4.22	−14.94	−1.03	3.19	3.46	7.86

[a] Structures in Figure S5 of SI. [b] Reference $E_{hydr} = -1423.229504E_h$. [c] Reference $E^{CP}_{hydr} = -1423.217421E_h$.

perpendicular to the six-membered ring, and the free H points away from the chiral H_{6a}, while the water molecule at O_{11} is fairly well conserved as in Eryc oi b, with the free hydrogens pointing downward for the water molecule at O_5 and upward for that at O_{11} (as in Bitu 1b).

In the ii b−/io b− complexes, the $O_5\cdots H_w$ and $O_{11}\cdots H_w$ separations are fairly similar, with the free H of the water molecule at O_5 and O_{11} pointing upward and downward, respectively, opposite to plain b. In the oi bd/oo bd complexes, the arrangement of the water molecule at O_5 is analogous to that assumed in oi bu and oo bu, whereas the $O_{11}\cdots H_w$ separation is almost exactly as in ii b−/io b− above. The free H of the water molecule at O_{11} points downward in both cases. Seemingly the variability in the water positions is very limited.

Interestingly, the stabilization due to hydration is almost independent of the solute conformation, as can be inferred by comparing the E_{hydr} values in each couple of similar water arrangements: ii bu and io bu, ii b− and io b−, oi bd and oo bd, and finally oi bu and oo bu. The 3-component counterpoise corrected hydration energies, reported in the last but one column of Table 8, show appreciable changes with respect to the uncorrected ones only when a water molecule is in close proximity to a prenyl group (an arrangement corresponding to large BSSE, see last column of Table 8), or far away from it. When water is bound to the ring oxygens, hydroxy group positions do not affect the CP-corrected results.

b. One Water Molecule per Hydroxy Group. In this case, it is necessary to distinguish whether the hydroxy group acts as a proton donor (acid) or as a proton acceptor (base). A simple graphical expedient is to add two letters to the label, indicating H or O, i.e., the binding site of the solute hydroxy group at C_3 and C_9 in this order for water.

The OH group hydration energies (ranging from −13.8 to −19.6 kcal/mol), reported with other quantities in Table 9, are more favorable on the average than those related to the ring O, although when behaving as a base on both OH groups E_{hydr} becomes −14.75 kcal/mol at most. In addition, in hydroxy··· water interactions, water prefers to behave as an H-bond acceptor, unless a nearby bulky group prevents its approach. In the last columns of Table 9, the 3-component counterpoise corrected hydration energies and BSSE are reported. BSSE corrections, discussed later on, show a significant variability in the systems considered according to OH group positions and water binding modes.

In the most favorably hydrated ii complex (HH), displayed in Figure 4a, the water molecules are located with their O along the solute hydroxy groups and one of their hydrogens pointing toward the prenyl group π density. The $O_w\cdots H$ separation is 1.78 Å whenever water behaves as a proton acceptor. When water acts as a proton donor (HO, shown in Figure 4b, OH, and OO) the $H_w\cdots O$ separation is longer (up to 2.02 Å). The water orientation relative to the OH group is conserved regardless which OH group is bound to and this occurs at each i OH group also in the other conformers.

TABLE 9: B3LYP/6-31G* Hydration Energies, Differential Solvent Effects, and Relative Energies of Hydration for a Water Molecule per Each Hydroxy Group of Erybraedin C (kcal/mol), Where Binding Sites for Water Are Also Indicated and Where BSSE and Counterpoise Corrected Relative Energies of Hydration Are Also Reported[a]

	ΔE_g	E_{hydr}	Δ(solv eff)	ΔE_{hydr}	ΔE^{CP}_{hydr}	−BSSE
Eryc ii (HH)[b]	0	−16.61	0	0[c]	0[d]	8.27
Eryc ii (HO)	0	−16.07	0.54	0.54	0.50	8.23
Eryc ii (OH)	0	−15.26	1.35	1.35	1.08	8.00
Eryc ii (OO)	0	−14.75	1.87	1.87	1.62	8.03
Eryc oi (HH)	2.04	−17.36	−0.75	1.29	−0.21	6.78
Eryc oi (HO)[b]	2.04	−17.53	−0.92	1.12	−1.57	5.58
Eryc oi (OH)	2.04	−14.13	2.48	4.52	4.81	8.57
Eryc io (HH)[b]	2.10	−18.38	−1.77	0.33	−1.52	6.42
Eryc io (OH)	2.10	−17.16	−0.54	1.56	−0.48	6.23
Eryc io (HO)	2.10	−15.65	0.96	3.06	2.95	8.15
Eryc io (OO)	2.10	−14.25	2.36	4.46	4.21	8.01
Eryc oo (HH)[b]	4.22	−19.61	−3.00	1.22	−2.59	4.46
Eryc oo (HO)	4.22	−17.16	−0.55	3.67	1.65	6.25
Eryc oo (OH)	4.22	−16.82	−0.21	4.01	2.03	6.29
Eryc oo (OO)	4.22	−13.76	2.85	7.07	6.88	8.08

[a] In parentheses, the first atom refers to the binding site for water onto the OH group at C_3, the second at C_9. [b] Structures (shown in Figure 4) subsequently embedded in the IEF−PCM continuum solvent (see section D.4). [c] Reference $E_{hydr} = -1423.233812E_h$. [d] Reference $E^{CP}_{hydr} = -1423.220631E_h$.

The oi complexes (only three of them are reported in Table 9) show a wide variety of hydrated structures, due to the steric hindrance lower than in ii. The $O_w\cdots H$ separation is 1.82 Å (just slightly longer than in ii), whenever water behaves as a proton acceptor. Water can bind with either lone pair to the o OH group, because the energy gap is very low (<0.2 kcal/mol). Water orientations and separations are conserved, in general, as before.

The most favorably dihydrated structure among those here considered is oo (HH). The water molecules are located with their O along the solute hydroxy groups and both their hydrogens point outward (Figure 4d). An analogous arrangement is maintained by each individual water in the oo (OH, HO) adducts. The same occurs for the water molecules behaving as proton donors, that keep their distance and orientation in the oo (OO, OH, HO) adducts. The $O_w\cdots H$ separations are invariably 1.82 Å (as for oi) whenever water behaves as a proton acceptor and the $H_w\cdots O$ ones range from 1.95 to 1.97 Å, when water acts as a proton donor (HO, OH, OO).

It is worth noting that there is a remarkable water stabilizing effect when one or both hydroxy group points outward (oi, io, and oo). In this way, io (HH), displayed in Figure 4c, turns out to be just 0.3 kcal/mol less stable than ii, despite its high internal energy in the gas phase. oi (HO) and oo (HH) are less stable than ii by about 1 kcal/mol. It is therefore likely that considering structures with low stability in vacuo or including other corrections, more favorable hydration energies can be obtained.

The relative stabilities of the four main conformers considered for erybraedin are reported in Figure 5.

The trend of total solvation free energies from IEF−PCM calculations in water almost coincides with the gas phase relative

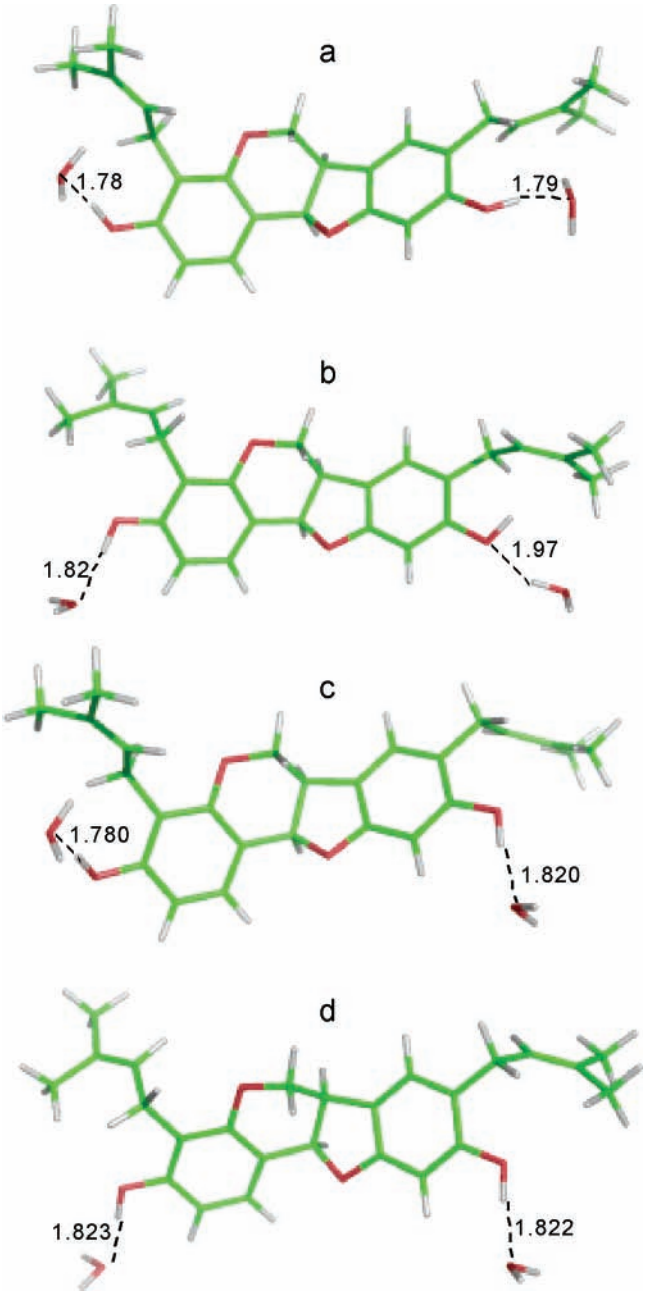

Figure 4. B3LYP/6-31G* optimized adducts of erybraedin C with one water molecule per hydroxy group (distances in Å): (a) Eryc ii (HH); (b) Eryc oi (HO); (c) Eryc io (HH); (d) Eryc oo (HH).

energies, although the electrostatic solvent effect is more favorable for the solvent exposed solute structures than the total solvent effect. In those cases, however, larger cavitation terms counterbalance electrostatic contributions, as already mentioned. In contrast to the continuum solvent, two explicit waters (long dashes, squares) may affect the relative stability of particular adducts at least.

(3) Counterpoise Corrections to a Number of Erybraedin Dihydrated Adducts. The inclusion of CP corrections to the hydration energies when water is bound to the ring O does not produce considerable changes to the relative hydration energies (see Table 8), because BSSE are almost constant, although large, regardless which solute/solvent arrangement is considered. Some differential effects can be found if the partner mutual position allows or not a significant overlap between the prenyl group and water charge distributions. In contrast, CP corrections remarkably affect the relative stabilities of specific adducts to the solute hydroxy groups (see Table 9), because for this kind of interaction BSSE vary depending on the complex arrangement. For the ii family adducts, BSSE are large and decidedly constant, ranging from −8.27 to −8.00 kcal/mol for HH and OH, respectively. For some adducts to the outward groups, conversely, they decrease significantly, because the water molecules are further apart from the solute, as is the case for the oo family. Even there, however, BSSE depend on the water positions as can be inferred examining Figure 4, where structures with a different amount of BSSE are shown. Therefore, CP-corrections allow a noticeable stability to be recovered for particular adducts, such as oo (HH), with respect to ii. To a minor extent, some adducts in the oi and io families as well turn out to be more favored than ii. The CP-corrected plot for the systems of Figure 5 is displayed in Figure 6.

TABLE 10: B3LYP/IEF−PCM/6-31G* Free Energy of Solvation and Solvent Effects (kcal/mol) on Dihydrated Structures of Erybraedin C Where Erybraedin Relative Energy in the Presence of Two Water Molecules Is Reported for Comparison and the Binding Sites for Water Are Also Indicated[a]

	ΔE_{hydr}	$^1/_2E_{susv}$	G^{es}(sol)	G^{tot}(sol)	ΔG_{es}	ΔG_{tot}
Eryc ii (HH)	0	−18.48	−15.98	−3.19	0[b]	0[c]
Eryc oi (HO)	1.12	−19.43	−16.77	−2.62	0.33	1.69
Eryc io (HH)	0.33	−19.87	−17.48	−3.88	−1.17	−0.36
Eryc oo (HH)	1.22	−22.27	−19.69	−5.53	−2.19	−1.12

[a] The first atom in parentheses refers to the binding site for water onto the OH group at C_3, the second at C_9 (the starting arrangements for B3LYP/IEF−PCM/6-31G* geometry optimizations in solution are displayed in Figure 4). [b] The reference free energy is $G_{es} = -1423.259275E_h$. [c] The reference free energy is $G_{tot} = -1423.238895E_h$.

(4) Dihydrated Structures of Erybraedin C Flexibly Embedded in a Continuum Solvent. As anticipated in Table 9, four dihydrated structures of erybraedin have been embedded in the IEF−PCM continuum solvent allowing the structures to relax. The structures, however, remain in arrangements similar to the starting ones, although they can change by several degrees. The results obtained are reported in Table 10.

As already put forward in the case of continuum solvation of the solute alone, the electrostatic solvent effect, when not completely counterbalanced by nonelectrostatic terms as in Eryc io and oo (HH), produces a significant stabilization of the dihydrated structures, as shown in Figure 6. In the case of Eryc oi (HO), on the contrary, nonelectrostatic terms prevail, thus destabilizing that peculiar adduct in water. However, it turns out evident from Figure 6 that both bulk solvent effects and counterpoise corrections favor solvent exposed arrangements of polar groups, thus indicating, as expected, that extended structures should be present in solution or in receptor sites.

(5) Four Water Molecules around Erybraedin. When four water molecules are added to erybraedin C, during the optimization they gather in pairs H-bonded to each other around the OH group regardless their initial positions. Reference is made to the water molecule H-bonded to the erybraedin hydroxy H as w1 (proton acceptor), while the water molecule donating its proton to the erybraedin hydroxy O is named w2. In this case, besides the energetic quantities displayed for previous adducts, the water−water interaction energy is reported to evaluate how much that contribution varies from an arrangement to the other.

In the Eryc ii adduct (Figure S6a in the Supporting Information), w1 at C_3 ($H\cdots O_{w1} = 1.74$ Å) is located between the OH group and the prenyl side chain. As a proton acceptor, however, instead of the π density, prefers w2 ($H_{w1}\cdots O_{w2} = 1.85$ Å) which is donating its proton to the hydroxy O ($H_{w2}\cdots O = 1.95$ Å). The water arrangement is similar for the hydroxy group at C_9.

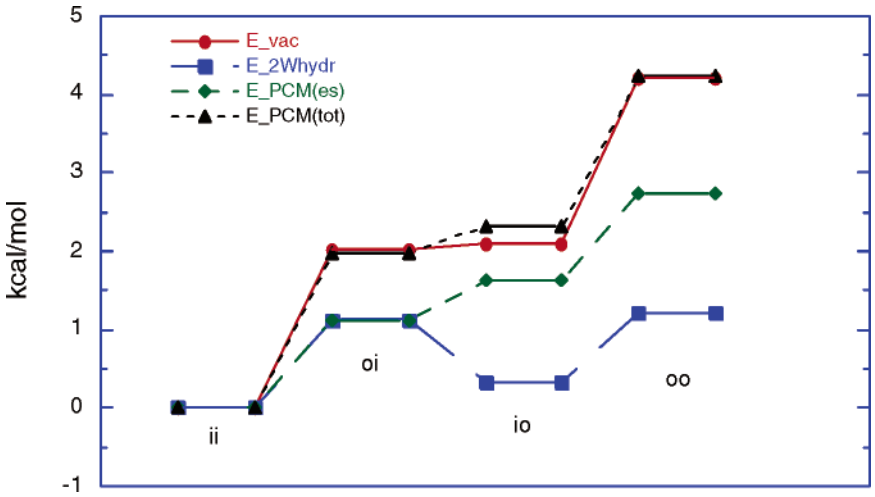

Figure 5. B3LYP/6-31G* relative stabilities of the four main conformers of erybraedin in vacuo (circles), in the (HH) dihydrated adducts (squares) and in aqueous solution (IEF−PCM: electrostatic and total components are marked with diamonds and triangles, respectively).

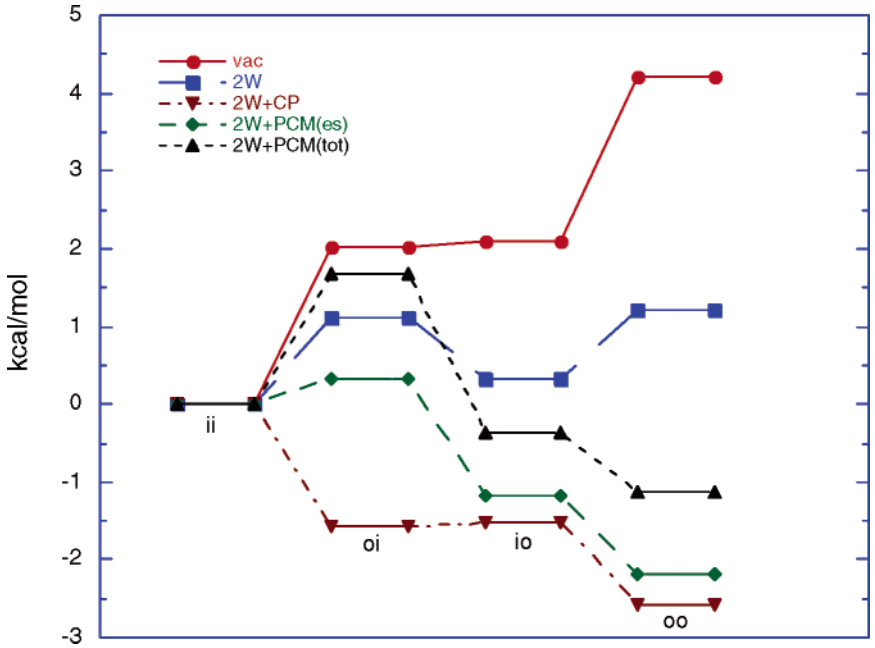

Figure 6. B3LYP/6-31G* relative stabilities of the four main conformers of erybraedin C in the (HH) dihydrated adducts (squares), with the inclusion of counterpoise corrections (down triangles), or when embedded in aqueous solution (IEF−PCM: electrostatic and total components are marked with diamonds and triangles, respectively). The in vacuo relative stabilities are also reported for comparison (circles).

TABLE 11: B3LYP/6-31G* Hydration Energy, Water−Water Interaction Energy, Differential Solvent Effect, and Relative Energy of Hydration (kcal/mol) for Erybraedin C Plus Four Water Molecules[a]

	ΔE_g	E_{hydr}	w−w inter energ	Δ(solv eff)	ΔE_{hydr}
Eryc ii	0	−43.58	−13.72	0	0[b]
Eryc oi	2.04	−45.56	−13.77	−1.98	0.06
Eryc oi (m)	2.24	−45.93	−13.66	−2.35	−0.11
Eryc io	2.10	−47.46	−14.56	−3.88	−1.77
Eryc oo	4.22	−49.93	−14.51	−6.35	−2.13

[a] Structures in Figure S6 of SI. [b] Reference $E_{hydr} = -1576.094698 E_h$.

This arrangement is roughly maintained in Eryc oi (Figure S6b), whereas at C_3 the outward orientation of the OH group significantly stabilizes the system, that becomes nearly as stable as the aforementioned Eryc ii adduct, as can be derived from the results reported in Table 11. Interestingly enough, when the starting orientation of the vicinal prenyl side chain is taken as in Eryc oo, the hydrated compound (Eryc oi (m), Figure S6c) becomes even somewhat more stable than the Eryc ii adduct described above.

In the Eryc io adduct (Figure S6d), the water arrangement at C_3 is similar as that found in Eryc ii, while the w2 arrangement at C_9 features a mutual position with respect to the vicinal prenyl side chain consistent with that found in Eryc oi (m), thus affecting accordingly the orientation of w1. In the Eryc oo adduct (Figure S6e), the remarkable exposition to the solvent of both hydroxy groups favors a prominent solvent stabilization of the oo erybraedin structure, as expected from our earlier study.[11] In the case presented, w1 at C_3 points its free H to the left-hand side and donates its proton to w2 located toward the observer. w2 in turn is H-bonded to the hydroxy O, with its free H pointing to the right-hand side. The situation is similar for the hydroxy group at C_9 with the water molecules placed in a roughly mirror arrangement with respect to those at C_3.

It should be noted, however, that we do not claim to have considered all the possible solvated structures of erybraedin, because the presence of at least 16 minima per each OH group

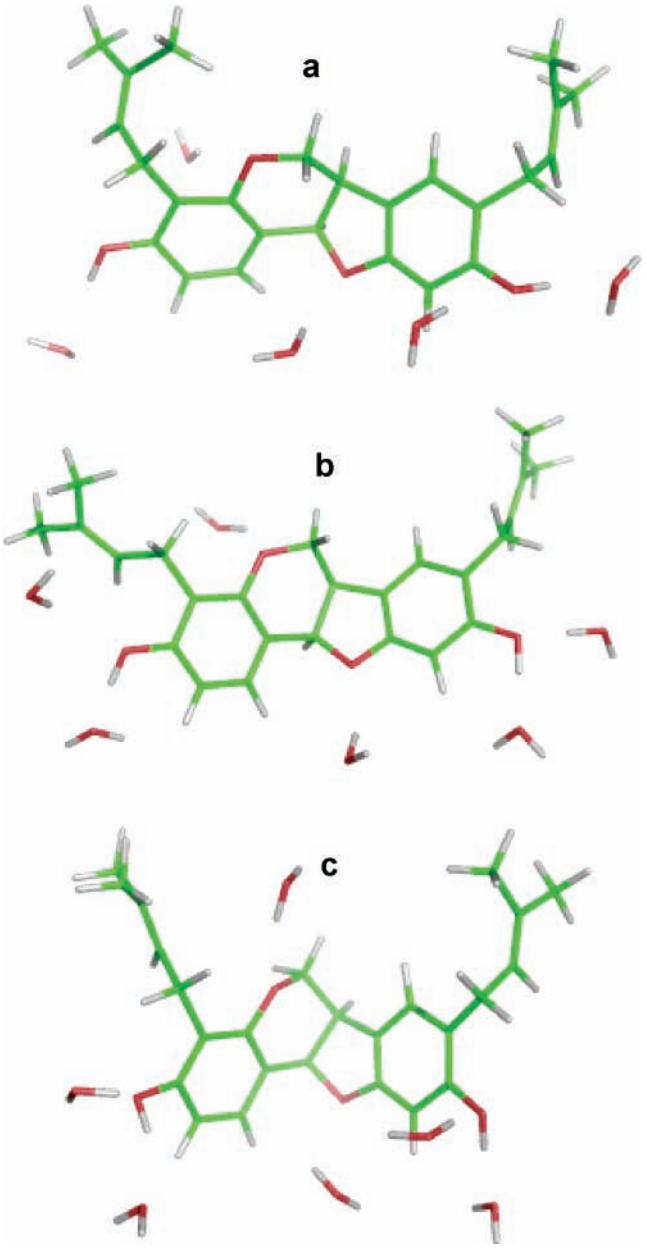

Figure 7. Snapshots along the trajectory of a molecular dynamics simulation in water (displaying water molecules within ~3 Å only of any polar atom of erybraedin) after (a) 100 ps, (b) 500 ps, and (c) 1 ns. (Data from ref 15.)

arrangement (not to mention possible other orientations of the side chains)[34] actually prevents this achievement. Furthermore, the H-bonding of water molecules in the first hydration shell between themselves is likely an artifact with respect to a real solution. For both these issues, we have taken into account a number of structures from snapshots along trajectories of molecular dynamics simulations in water[15] of this compound.

E. Explicit Water Molecules from MD Simulations. *a.* To examine the hydration pattern of explicit water molecules about erybraedin in aqueous solution and the relevant stabilization energy, three different structures, displayed in Figure 7, have been considered.[35] As can be inferred from Figure 7, only the water molecules close to the polar groups in the solute (ring O and OH groups) have been included in the calculations (altogether or four/two at a time).

The strategy employed is as follows: B3LYP/6-31G* single point calculations in vacuo have been carried out on (1) the system as a whole; (2) the solute plus two water molecules, one per each ring oxygens; (3) the solute plus two water molecules, one per each hydroxy groups; (4) the solute plus four water molecules, two per each hydroxy groups (when possible); (5) the individual molecules according to the need (solute, all the water molecules as in point 1, two/four water molecules as in points 2−4. The aforementioned calculations in points 1−4 have been carried out also at the B3LYP/IEF−PCM/6-31G* level with each system embedded in the solvent as a continuum to account for bulk solvent effects.

TABLE 12: B3LYP/6-31G* Hydration Energies (kcal/mol) from Single Point Calculations of Erybraedin−Water Adducts from Snapshots along an MD Trajectory.[a] Relative Internal Energies for Erybraedin and Interaction Energies among Solvent Molecules Are Also Reported

			E_{hydr}			
Eryc	ΔE_{su}	ΔE_{sv}	(*n*) *n*H_2O	$4H_2O$ at OH	$2H_2O$ (HO)	$2H_2O$ (ring O)
100 ps	53.69	−0.02	(5) −19.85		−13.89	−3.75
500 ps	51.64	−0.49	(6) −30.24	−22.25	−13.09	−7.67
1 ns	70.00	−1.57	(6) −29.40	−22.99	−15.73	−6.57

[a] The values in Hartrees (E_h) used to compute E_{hydr} are reported below (Table 12).

Of course, belonging to a snapshot along a molecular dynamics simulation, the structures are not local minima. Especially the solute can be remarkably distorted with respect to its equilibrium geometry at the B3LYP/6-31G* level. The OH groups, in particular, are rather solvent exposed although a limited number of H-bonding water molecules are found around them. Purpose of these calculations, however, is not to obtain values comparable with the purely quantum mechanical ones, as when simulated annealing is subsequently carried out on each snapshot.[36] Conversely, we wish to include the hydration contribution of weakly H-bonded water molecules (because not perfectly aligned or slightly further apart) about flexible structures to avoid known problems with continuum solvent models,[37] tending to privilege the structures more stable in vacuo,[38] as shown also above. Other authors prefer using dynamics to mainly sample intermolecular interactions about small solutes.[39]

Pterocarpans indeed, despite the rigid aspect of their scaffold, are flexible not only due to their substituents but because of the presence of a CH_2 group in the six-membered ring. Interestingly, in the 1 ns frame erybraedin belongs to the O_t type, significantly bent (see Figure S7a of the Supporting Information) with respect to the H_t ones, preventing water molecules from entering inside the blades formed by the fused ring system.

Relative internal energies of the solute structures and interaction energies among all solvent molecules considered (ΔE_{su} and ΔE_{sv}, respectively) are reported in Table 12, together with total (all the water molecules taken into account are included in the calculation) and partial hydration energies.[40]

Despite the energy gaps of the solute arrangements considered with respect to its local minima and the far-from-perfect H-bond alignments of water molecules, the hydration energy is favorable enough. The hydration energy due to four water molecules about the OH groups (amounting to about −30 kcal/mol from Table 10) turns out to be about −23 kcal/mol, with a very limited contribution from water−water interactions. In the 500 ps frame the $4H_2O$ interaction energy is only −0.35 kcal/mol, taking into account that there is a repulsive interaction by 0.34 kcal/mol between the proton acceptors alone (constant in the three situations). Conversely, the terms related to the water molecules bound to the ring O are somewhat different in the 100, 500,

TABLE 13: B3LYP/IEF−PCM/6-31G* Electrostatic and Total Free Energies of Solvation (kcal/mol) on the Hydrated Structures of Erybraedin C Taken from the MD Snapshots of Table 12

Eryc	E_g (E_h)	G^{es}(sol)	G^{tot}(sol)
100 $5H_2O$	−1652.380305	−30.49	−5.86
100 $2H_2O$ (HO)	−1423.143367	−19.96	−4.70
100 $2H_2O$ (ring O)	−1423.127608	−18.76	−1.93
500 $6H_2O$	−1728.809825	−33.00	−6.05
500 $4H_2O$ at OH	−1575.978958	−26.80	−7.03
500 $2H_2O$ (HO)	−1423.145350	−19.46	−6.20
500 $2H_2O$ (ring O)	−1423.136666	−18.76	−2.68
1 ns $6H_2O$	−1728.780950	−32.90	−3.73
1 ns $4H_2O$ at OH	−1575.954061	−26.05	−4.30
1 ns $2H_2O$ (HO)	−1423.120324	−19.82	−5.15
1 ns $2H_2O$ (ring O)	−1423.105555	−18.63	−1.58

and 1000 ps frames, ranging from 0.09 to 0.38 and 0.44 kcal/mol, respectively. The O_t scaffold arrangement in the 1 ns frame keeps the solvent molecules closer to each other than in the H_t structures. The interaction energy among the four water molecules, therefore, turns out to be −2.34 kcal/mol, considering the aforementioned repulsive interaction between the proton acceptors alone.

b. Bulk Solvent Effects. A continuum solvent ($\epsilon = 78.39$) has been used to solvate the hydrated clusters of erybraedin considered thus far. The systems considered, named according to the headers of Table 12, are reported in Table 13, together with their B3LYP/6-31G* energy in vacuo, used to compute E_{hydr} in Table 12.

The presence of water molecules around the solute significantly enhances the solvent effect, as might be expected. What is interesting here, is that the total solvent effect is remarkably different despite close values in the electrostatic contributions, such as those found when dihydrated adducts are considered. In that case, for water molecules H-bonded to ring oxygens and OH groups, respectively, total values in the −6.2 to −5.2 and −2.7 to −1.6 kcal/mol ranges correspond to analogous electrostatic contributions (−19/−20 kcal/mol). Total values in the upper range are obtained when more than two water molecules are considered, although the 1 ns frame represents a partial exception.

F. Structures Optimized Starting from a Frame along the MD Simulation. A number of additional calculations have been carried out for erybraedin using the 500 ps frame as a test case. B3LYP/6-31G* geometry optimizations starting from the structures assumed in the 500 ps frame have been performed in vacuo for the isolated solute and the dihydrated solute. For both initial systems geometry optimizations in the presence of the continuum solvent have been carried out as well (B3LYP/ IEF−PCM/6-31G* level).

It is noteworthy first of all that the local minimum reached in the isolated solute optimization is of the oo type (see Figure S7b in the Supporting Information) with a value of φ_5 (160°, starting from 118°) different from those obtained thus far for oo (±90°). The relative energy of this structure is 4.10 kcal/mol, slightly better than that (4.22 kcal/mol) obtained for the oo structure by coupling all the stable dihedral values. It is however well-known that minimization at fixed intervals along a segment of dynamics is a powerful conformational sampling technique.[41]

The optimized dihydrated cluster features a solute structure analogous to the aforementioned one, with $\varphi_5 = 156°$. Both water molecules are located with one of the O lone pairs directed toward the hydroxy H at an $O_w\cdots H$ separation of 1.82 Å with the $O_w\cdots HO$ angle of 172° although starting from different positions.

The continuum solvent does not prevent the solute or water molecules from assuming the structure described above. The variations are very limited ($\varphi_5 = 160°$ vs 156° for the solute alone or its dihydrated form embedded in the continuum), while both water molecules end at 1.75 Å with the $O_w\cdots HO$ angle of 177°. The continuum solvent effect is more favorable by 0.39 kcal/mol on the structure optimized starting from the MD simulation than using Eryc oo. For the dihydrated adduct an even better result (−1.85 vs −1.12 kcal/mol) is obtained.

IV. Conclusions

A systematic study has been carried out on the solvation properties of (*R*,*R*)-bitucarpin A and erybraedin C. To this end, the local minimum structures in vacuo for each OH arrangement of erybraedin have been located exploiting the minimum energy values for the prenyl side chain dihedrals of bitucarpin ($\varphi_3 \approx \pm 90$, $\varphi_4 \approx \pm 120°$). The situation however can be somewhat different for a prenyl side chain at C_8, as can be inferred from the structure obtained via minimization of a solute geometry along an MD trajectory. The inclusion of zero point, thermal and entropy effects leaves mutual stabilities practically unaltered.

The continuum solvent effect at the B3LYP/IEF−PCM/6-31G* level on the relaxed solute in aqueous solution is almost insensitive in bitucarpin and very limited in erybraedin, either considering the H_t/O_t backbone arrangements or their interconversion transition states.

Clusters obtained adding explicit water molecules in the supermolecule framework allow determination of preferential hydration sites. The affinity of water for the methoxy oxygens of bitucarpin is slightly feebler than that for the ring oxygens. The interaction energy with water, however, does not appreciably modify the mutual stabilities of the various adducts when water molecules are H-bonded to methoxy oxygens, whereas a particular adduct to the ring oxygens of the minimum energy conformer is favored. In the case of erybraedin, some oi and oo rotamers are remarkably stabilized because of water molecules bound to ring oxygens, although without affecting the stability order. When water molecules act as proton donors toward hydroxy oxygens, the hydration energy is constantly somewhat more favorable than toward ring oxygens. The best hydration site is however the hydroxy hydrogen, because the hydroxy group prefers acting as a proton donor, unless steric hindrance prevents water from approaching. This kind of adducts (HH) significantly stabilizes the erybraedin io and oo rotamers rendering them about as stable as the ii and oi ones, respectively. Embedding the dihydrated structures in the continuum solvent, thus taking into account bulk solvent effects, further stabilizes the io and oo rotamers of erybraedin, that become the most stable ones. This effect should also be enhanced, because counterpoise corrections sharply favor some water adducts to the OH groups belonging to the oo family, followed by the oi and io ones. Thus, solvent exposed structures become the most stable ones, as we hypothesized earlier.[11]

When two water molecules per each erybraedin OH group are included in the calculations, they H-bond to each other and to the solute OH group. To avoid this artifact, structures derived from previous MD simulations have been used. Starting from an MD derived arrangement, geometry optimization in vacuo produced a rotamer not found during the systematic combination of stable dihedral values. The dihydrated form of this structure, corresponding to an oo erybraedin rotamer as well, is remarkably stabilized in the continuum solvent.

The results presented confirm the importance of taking into account specific H-bonding interactions in protic solvents,

supplemented by bulk solvent effects computed in the polarizable continuum solvent framework. Counterpoise corrections play a prominent role, because they depend on peculiar arrangements of solute−water adducts.

Acknowledgment. We are grateful to S. Monti for granting us permission to use joint data (3 structures from earlier MD simulations).

Supporting Information Available: View of a bush of *Psoralea bituminosa* (Figure S1), molecular electrostatic potential from RESP charges (ref 15) around Bitu 1, Eryc ii, and Eryc oo (Figure S2 a-c), B3LYP/6-31G* adducts of bitucarpin A with one water molecule per methoxy group (Figures S3 a−h); B3LYP/6-31G* adducts of bitucarpin A with one water molecule per ring O (Figures S4 a−j), B3LYP/6-31G* adducts of erybraedin C with one water molecule per ring O (Figures S5 a−j), B3LYP/6-31G* adducts of erybraedin C with two water molecules per hydroxy group (Figures S6 a−e), a different view of the 1 ns snapshot, shown in Figure 6c (Figure S7a), B3LYP/6-31G* optimized structure starting from the solute geometry in the 500 ps frame (Figure S7b), B3LYP/6-31G* relative stabilities, a few geometric parameters of the ii, oi, io and oo local minima of erybraedin C (Tables S1−S4) and a table of Cartesian coordinates of the structures displayed in Figure 1. This material is available free of charge via the Internet at http://pubs.acs.org.

References and Notes

(1) Casagrande, F.; Darbon J. M. *Biochem. Pharmacol.* **2001**, *61*, 1205.

(2) (a) Dixon, R. A.; Achnine, L.; Kota, P.; Liu, C.-J.; Reddy, M. S. S.; Wang, L. *Mol. Plant. Pathology* **2002**, *3*, 371. (b) Durango, D.; Quiñones, W.; Torres, F.; Rosero, Y.; Gil, J.; Echeverri, F. *Molecules* **2002**, *7*, 817. (c) Dewick, P. M.; Steel, M. J. *Phytochemistry* **1982**, *21*, 1599. (d) VanEtten, H. D. **1976** *Phytochemistry 15*, 655. (e) Kuc, J. *Annu. Rev. Phytopathol.* **1972**, *10*, 207.

(3) (a) Latha, P. G.; Evans, D. A.; Panikkar, K. R.; Jayavardhanan, K. K. *Fitoterapia* **2000**, *71*, 223. (b) Dev, S. *Environ. Health Perspect.* **1999**, *107*, 783. (c) Mitscher, L. A.; Simon, K.; Gollapudi, S. R.; Okwute, S. K. *J. Nat. Prod.* **1987**, *50*, 1025. (d) Gottlieb, O. R. *J. Ethnopharmacol.* **1979**, *1*, 309.

(4) (a) Bojase, G.; Majinda, R. R.; Gashe, B. A.; Wanjala, C. C. *Planta Med.* **2002**, *68*, 615. (b) Mundodi, S. R.; Watson, B. S.; Lopez-Meyer, M.; Paiva, N. L. *Plant Mol. Biol.* **2001**, *46*, 421. (c) Majinda, R. R. T.; Abegaz, B. M.; Bezabih, M.; Ngadjui, B.; Wanjala, C. C. W.; Mdee, L. K.; Bojase, G.; Silayo, A.; Masesane, I.; Yeboah, S. O. *Pure Appl. Chem.* **2001**, *73*, 1197. (d) Garcez, W. S.; Martins, D.; Garcez, F. R.; Marques, M. R.; Pereira, A. A.; Oliveira, L. A.; Rondon, J. N.; Peruca, A. D. *J. Agric. Food Chem.* **2000**, *48*, 3662. (e) Máximo, P.; Lourenço, A.; Savluchinske Feio, S.; Roseiro, J. C. *Z. Naturforsch.* **2000**, *55c*, 506. (f) Nkengfack, A. E.; Vouffo, T. W.; Fomum, Z. T.; Meyer, M.; Bergendorff, O.; Sterner, O. *Phytochemistry* **1994**, *36*, 1047. (g) Hadwiger, L. A.; Ogawa, T.; Kuyama, H. *Mol. Plant-Microbe Interact.* **1994**, *7*, 531. (h) Bandara, B. M.; Kumar, N. S.; Samaranayake, K. M. *J. Ethnopharmacol.* **1989**, *25*, 73.

(5) (a) Sato, M.; Tanaka, H.; Oh-Uchi, T.; Fukai, T.; Etoh, H.; Yamaguchi, R. *Phytother. Res.* **2004**, *18*, 906. (b) Yin, S.; Fan, C. Q.; Wang, Y.; Dong, L.; Yue, J. M. *Bioorg. Med. Chem.* **2004**, *12*, 4387. (c) Tanaka, H.; Oh-Uchi, T.; Etoh, H.; Sako, M.; Asai, F.; Fukai, T.; Sato, M.; Murata, J.; Tateishi, Y. *Phytochemistry* **2003**, *64*, 753. (d) Sato, M.; Tanaka, H.; Fujiwara, S.; Hirata, M.; Yamaguchi, R.; Etoh, H.; Tokuda, C. *Phytomedicine* **2003**, *10*, 427. (e) Fukai, T.; Marumo, A.; Kaitou, K.; Kanda, T.; Terada, S.; Nomura, T. *Life Sci.* **2002**, *71*, 1449. (f) Ahamd, W.-Y.; Said, I. M.; Soon, S.-Y.; Takayama, H.; Kitajima, M.; Aimi, N. *OnLine J. Biol. Sci.* **2002**, *2*, 542. (g) Nkengfack, A. E.; Vardamides, J. C.; Fomum, Z. T.; Meyer, M. *Phytochemistry* **1995**, *40*, 1803. (h) Mitscher, L. A.; Okwute, S. K.; Gollapudi, S. R.; Drake, S.; Avona, E. *Phytochemistry* **1988**, *27*, 3449.

(6) (a) Palazzino, G.; Rasoanaivo, P.; Federici, E.; Nicoletti, M.; Galeffi, C. *Phytochemistry* **2003**, *63*, 471. (b) Blatt, C. T.; Chavez, D.; Chai, H.; Graham, J. G.; Cabieses, F.; Farnsworth, N. R.; Cordell, G. A.; Pezzuto, J. M.; Kinghorn, A. D. *Phytother. Res.* **2002**, *16*, 320. (c) da Silva, A. J.; Buarque, C. D.; Brito, F. V.; Aurelian, L.; Macedo, L. F.; Malkas, L. H.; Hickey, R. J.; Lopes, D. V.; Noel, F.; Murakami, Y. L.; Silva, N. M.; Melo, P. A.; Caruso, R. R.; Castro, N. G.; Costa, P. R. *Bioorg. Med. Chem.* **2002**, *10*, 2731. (d) Seo, E. K.; Kim, N. C.; Mi, Q.; Chai, H.; Wani, M. E.; Navarro, H. A.; Burgess, J. P.; Graham, J. G.; Cabieses, F.; Tan, G. T.; Farnsworth, N. R.; Pezzuto, J. M.; Kinghorn, A. D. *J. Nat. Prod.* **2001**, *64*, 1483. (e) Fukai, T.; Sakagami, H.; Toguchi, M.; Takayama, F. Iwakura, I.; Atsumi, T.; Ueha, T.; Nakashima, H.; Nomura, T. *Anticancer Res.* **2000**, *20*, 2525. (f) Alvarez, L.; Rios, M. Y.; Esquivel, C.; Chavez, M. I.; Delgado, G.; Aguilar, M. I.; Villareal, M. L.; Navarro, V. *J. Nat. Prod.* **1998**, *61*, 767. (g) Chaudhuri, S. K.; Huang, L.; Fullas, F.; Brown, D. M.; Wani, M. C.; Wall, M. E. *J. Nat. Prod.* **1995**, *58*, 1966. (h) Dagne, E.; Gunatilaka, A. A.; Kingston, D. G.; Alemu, M.; Hofmann, G.; Johnson, R. K. *J. Nat. Prod.* **1993**, *56*, 1831. (i) Skinnider, L.; Stoessl, A. *Experientia* **1986**, *42*, 568.

(7) (a) McKee, T. C.; Bokesch, H. R.; McCormick, J. L.; Rashid, M. A.; Spielvogel, D.; Gustafson, K. R.; Alavanja, M. M.; Cardelline, J. H., II; Boyd, M. R. *J. Nat. Prod.* **1997**, *60*, 431. (b) Engler, T. A.; La Tessa, K. O.; Iyengar, R.; Chai, W.; Agrios, K. *Bioorg. Med. Chem.* **1996**, *4*, 1755. (c) Engler, T. A.; Lynch, K. O.; Reddy, J. P.; Gregory, G. S. *Bioorg. Med. Chem. Lett.* **1993**, *3*, 1229.

(8) (a) da Silva, A. J.; Coelho, A. L.; Simas, A. B.; Moraes, R. A.; Pinheiro, D. A.; Fernandes, F. F.; Arruda, E. Z.; Costa, P. R.; Melo, P. A. *Bioorg. Med. Chem. Lett.* **2004**, *14*, 431. (b) Reyes-Chilpa, R.; Gomez-Garibay, F.; Quijano, L.; Magos-Guerrero, G. A.; Rios, T. *J. Ethnopharmacol.* **1994**, *42*, 199.

(9) Maurich, T.; Pistelli, L.; Turchi, G. *Mut. Res.* **2004**, *561*, 75.

(10) Cottiglia, F.; Casu, L.; Bonsignore, L.; Casu, M.; Floris, C.; Leonti, M.; Gertsch, J.; Heilmann, J. *Planta Med.* **2005**, *71*, 254.

(11) Alagona, G.; Ghio, C.; Monti, S. *Phys. Chem. Chem. Phys.* **2004**, *6*, 2849.

(12) (a) Miertus, S.; Scrocco, E.; Tomasi, J. *Chem. Phys.* **1981**, *55*, 117. (b) Tomasi, J.; Persico, M. *Chem. Rev.* **1994**, *94*, 2027. (c) Barone, V.; Cossi, M.; Tomasi, J. *J. Chem. Phys.* **1997**, *107*, 3210. (d) Cramer, C. J.; Truhlar, D. G. In *Solvent Effects and Chemical Reactivity*; Tapia, O., Bertrán, J., Eds.; Kluwer: Dordrecht, The Netherlands, 1996; p 1.

(13) (a) Cancès, E.; Mennucci, B.; Tomasi, J. *J. Chem. Phys.* **1997**, *107*, 3032. (b) Cancès, E.; Mennucci, B. *J. Chem. Phys.* **1998**, *109*, 249. (c) Cancès, E.; Mennucci, B. *J. Chem. Phys.* **1998**, *109*, 260.

(14) Clusters involving more than one water molecule per hydration site have also been taken from snapshots along trajectories obtained during previous molecular dynamics simulations.[15]

(15) Alagona, G.; Ghio, C.; Monti, S. *J. Phys. Chem. B*, **2005**, *109*, 16918.

(16) Abkowicz-Bienko, A.; Biczysko, M.; Latajka, Z. *Comput. Chem.* **2000**, *24*, 303.

(17) (a) Lee, C.; Yang, W.; Parr, R. G. *Phys. Rev. B* **1988**, *37*, 785. (b) Becke, A. D. *J. Chem. Phys.* **1993**, *98*, 5648.

(18) Hehre, W. J.; Radom, L.; Schleyer, P. v. R.; Pople, J. A. *Ab Initio Molecular Orbital Theory*; Wiley: New York, 1986.

(19) Gaussian 03, Revision C.02. Frisch, M. J.; Trucks, G. W.; Schlegel, H. B.; Scuseria, G. E.; Robb, M. A.; Cheeseman, J. R.; Montgomery, J. A., Jr.; Vreven, T.; Kudin, K. N.; Burant, J. C.; Millam, J. M.; Iyengar, S. S.; Tomasi, J.; Barone, V.; Mennucci, B.; Cossi, M.; Scalmani, G.; Rega, N.; Petersson, G. A.; Nakatsuji, H.; Hada, M.; Ehara, M.; Toyota, K.; Fukuda, R.; Hasegawa, J.; Ishida, M.; Nakajima, T.; Honda, Y.; Kitao, O.; Nakai, H.; Klene, M.; Li, X.; Knox, J. E.; Hratchian, H. P.; Cross, J. B.; Bakken, V.; Adamo, C.; Jaramillo, J.; Gomperts, R.; Stratmann, R. E.; Yazyev, O.; Austin, A. J.; Cammi, R.; Pomelli, C.; Ochterski, J. W.; Ayala, P. Y.; Morokuma, K.; Voth, G. A.; Salvador, P.; Dannenberg, J. J.; Zakrzewski, V. G.; Dapprich, S.; Daniels, A. D.; Strain, M. C.; Farkas, O.; Malick, D. K.; Rabuck, A. D.; Raghavachari, K.; Foresman, J. B.; Ortiz, J. V.; Cui, Q.; Baboul, A. G.; Clifford, S.; Cioslowski, J.; Stefanov, B. B.; Liu, G.; Liashenko, A.; Piskorz, P.; Komaromi, I.; Martin, R. L.; Fox, D. J.; Keith, T.; Al-Laham, M. A.; Peng, C. Y.; Nanayakkara, A.; Challacombe, M.; Gill, P. M. W.; Johnson, B.; Chen, W.; Wong, M. W.; Gonzalez, C.; Pople, J. A. Gaussian, Inc.: Wallingford, CT, 2004.

(20) (a) Csaszar, P.; Pulay, P. *J. Mol. Struct. (THEOCHEM)* **1984**, *114*, 31. (b) Farkas, O.; Schlegel, H. B. *J. Chem. Phys.* **1999**, *111*, 10806.

(21) McQuarrie, D. A. *Statistical Mechanics*, University Science Books: Sausalito, CA, 2000.

(22) Amovilli, C.; Barone, V.; Cammi, R.; Cancès, E.; Cossi, M.; Mennucci, B.; Pomelli, C. S.; Tomasi, J. *Adv. Quantum Chem.* **1998**, *32*, 227.

(23) Bondi, A. *J. Phys. Chem.* **1964**, *68*, 441.

(24) Boys, S. F.; Bernardi, F. *Mol. Phys.* **1970**, *19*, 553.

(25) Sokalski, W. A.; Roszak, S.; Hariharan, P. C.; Kaufman, J. *Int. J. Quantum Chem.* **1983**, *23*, 847.

(26) Thus the geometry deformation treatment [Alagona, G.; Ghio, C.; Tomasi, S. *Theor. Chem. Acc.* **2004**, *111*, 287] does not need to be performed since both reference energies (in the basis set either of individual components or of the adduct) make use of the same geometry.

(27) Due to the steric and electrostatic hindrance of the inward pointing OH protons, it was frequently necessary to preliminarily perform energy minimizations constraining one of the prenyl side chains to keep positions close to the $\varphi_3 = \pm 90°$ and $\varphi_4 = \pm 120°$ values.

(28) The transition states are identified using the letters corresponding to the minima they join, going from top to bottom or from right to left, in any case.

(29) The TS along the map sides are actually eight, but the facing pairs are equal as occurs to the local minima.

(30) (a) Alagona, G.; Bonaccorsi, R.; Ghio, C.; Montagnani, R.; Tomasi, J. *Pure Appl. Chem.* **1988**, *60*, 231. (b) Alagona, G.; Ghio, C.; Igual, J.; Tomasi, J. *J. Am. Chem. Soc.* **1989**, *111*, 3417. (c) Alagona, G.; Ghio, C.; Igual, J.; Tomasi, J. *J. Mol. Struct. (THEOCHEM)* **1990**, *204*, 253. (d) Alagona, G.; Ghio, C. *J. Mol. Struct. (THEOCHEM)* **1992**, *254*, 287.

(31) (a) Pavone, M.; Benzi, C.; De Angelis, F.; Barone, V. *Chem. Phys. Lett.* **2004**, *395*, 120. (b) Benzi, C.; Crescenzi, O.; Pavone, M.; Barone, V. *Magn. Reson. Chem.* **2004**, *42*, S57. (c) Crescenzi, O.; Pavone, M.; De Angelis, F.; Barone, V. *J. Phys. Chem. B* **2005**, *109*, 445.

(32) Alagona, G.; Ghio, C. *Int. J. Quantum Chem.* **2002**, *90*, 641.

(33) Major changes are found for the a+ and a− structures, where the $H_w\cdots O_{11}$ distance/$O_wH_wO_{11}$ angle are 2.10 Å/149° and 2.02 Å/160°, respectively, with the H-bonded H_wO_w group almost perpendicular to the five membered heteroring.

(34) From B3LYP/6-31G* optimizations carried out starting from solute structures along the MD simulation trajectories of ref 15 an in plane arrangement ($\varphi_5 \approx \pm 180°$) of the prenyl group at C_8 turns out to be equal in energy to the almost perpendicular arrangement ($\varphi_5 \approx \pm 90°$).

(35) Specifically those after 100 ps, 500 ps, and 1 ns of molecular dynamics starting from the oo erybraedin structure; the last two structures, including however all the water molecules within 2.5 Å of any solute atom, are displayed in ref 15 (Figure 11).

(36) Alagona, G.; Ghio, C.; Monti, S. *Int. J. Quantum Chem.* **2002**, *88*, 133.

(37) Zhou, R.; Berne, B. J. *Proc. Natl. Acad. Sci. U.S.A.* **2002**, *99*, 12777.

(38) Nagy, P. I.; Alagona, G.; Ghio, C.; Takács-Novák, K. *J. Am. Chem. Soc.* **2003**, *125*, 2770.

(39) (a) Mennucci, B.; Martínez, J. M.; Tomasi, J. *J. Phys. Chem. A* **2001**, *105*, 7287. (b) Mennucci, B.; Martínez, J. M. *J. Phys. Chem. A* **2005**, *109*, 9818.

(40) Concerning partial hydration energies, $4H_2O$ at OH indicates both proton acceptor and donor water molecules at both OH groups, $2H_2O$ (HO) indicates proton acceptor water molecules (one for each OH group), and $2H_2O$ (ring O) indicates proton donor water molecules (one for each ring O).

(41) Alagona, G.; Ghio, C.; Monti, S. *Task Q.* **1998**, *2*, 563.